

THE HIGH-POWER ARC-JET PLASMA GENERATOR (PLASMA TORCH) CHARACTERISTICS AND PERFORMANCE

¹Sedanur Toraman, ²T. Yaşar Katırcıoğlu, ³Çağlar Terzi

¹MSc. Student, Metallurgical and Materials Engineering, ARTECS Anadolu R&D Technology Engineering and Consultancy Inc. Bahçelievler Mahallesi Ankara Üniversitesi Teknokent Binası D Blok No: 7 06830 Gölbaşı Ankara

²PhD., Chemistry, ARTECS Anadolu R&D Technology Engineering and Consultancy Inc.

³PhD. Candidate, Computer Engineering, ARTECS Anadolu R&D Technology Engineering and Consultancy Inc.

ABSTRACT

Nowadays, because of the unique and interesting features of plasmas, there is an increasingly wide range of applications in plasma technology. Plasmatron is an electro-technology device that converts electrical energy into heat energy. Medicine, energy, metallurgy, textile, aerospace technologies, thermochemical processes such as gasification and combustion processes are given examples of usage area of plasmatrons. In these processes, the plasmatron becomes an energy producer for the system and the requirement of hydrocarbon based fuel for combustion systems is eliminated. This paper highlights the importance of the characteristics and performance of the high-power arc-jet plasma torch and the diagnostics of plasma such as probes and other measurement devices to be used. In this study, as the plasma characteristics inside the plasmatron which means plasma parameters in the mixing chamber, pressure was directly measured, chamber temperature was calculated by using Gas Dynamic Method. In addition to the determination of internal parameters of plasmatron, two main intrusive measurement techniques which are the Pitot probe and the calorimetric heat flux probe were used in order to measure and characterize the plasmatron flame. In this paper, the main structure of a high-power plasma torch with power over 1 MW is summarized and the test methodology and the results obtained during the tests are also presented. The average values obtained at a power level about 1000 kW from our tests are given as following: the plasmatron chamber temperature above 4000 K, the plasmatron chamber pressure above 14.00 bar, and heat flux above 6.50 Mcal/kg·m².

Keywords: Plasmatron, High-power, Alternating Current Plasma, Coal, Solid Waste, Biomass, Burning, Gasification, Thermal Insulation Materials.

1. INTRODUCTION

In recent years, there are many investigations about the design and the development of the plasmatron facility because of a wide range of usage area of plasmatrons. Arc jet plasma generated by heating the gas through an electric discharge between electrodes is used recently in Europe, USA, and Russia. The von Karman Institute (VKI) designed an inductively-coupled plasma wind tunnel which uses a high frequency, high power and high voltage solid state (MOS technology) [1]. Furthermore, at NASA's Ames Research Center in California, SLA- 561 was tested in the plasma arc facility [2]. In Keldysh Research Center (KeRC, Moscow), a new design of three-phase AC plasmatron was developed, and the details of this systems are given in the KeRC experts' article [3]. The high-power plasma arc system is being one of the main alternatives to substitute current fuel oil based ignitor or burning system for solid waste and low-quality coal burning or gasification. Plasma application in the production of synthesis gas and hydrogen creates an attractive alternative to conventional thermo-catalytic technologies [4]. Until 2008, more than ninety plasma combustion systems have been installed in Russia, Kazakhstan, and Ukraine. Plasma combustion system allows high-quality domestic coal and biomass resources to be burned under appropriate conditions and high efficiency in power plants thanks to high temperature and plasma [5]. Also, plasma innovation can be effectively

adjusted in the treatment of different wastes such as municipal solid wastes, heavy oil, used car tires and medical wastes. Thus, it is considered to be an extremely attractive way of processing of waste-to-energy [6].

Depending on the purpose, various types of plasmatrons have been developed. These plasmatrons show a great variety of current alternatives. It is the most widely used direct current (DC) plasmatrons for different operations on metals. In alternating current (AC) plasmatrons, the gas flow is heated by AC electric arc. Generally, alternating current plasmatrons have been used more extensively, especially in high-power plasmas, instead of DC plasma torches. According to the desired stabilization value of the plasma in AC arc plasmatrons, power is stabilized and regulated by the inductance coils (reactors). This system simplifies the electrical circuitry and diminishes the cost because it removes the need for direct current supply [7]. In addition, some of the advantages and features of AC arc plasmatrons over DC supplies are listed as follows:

- For the power of the Megawatt range, the DC source units are quite complex, space-consuming and costly. For AC arc plasmatrons, special power supply devices are not required but they can be operated in an industrial three-phase electric power line. In addition to the absence of power

cap, the switching equipment on the line is simple and reliable.

- In DC arc plasmatrons, the cathode lifetime is much lower than in AC ones. In the AC arc plasmatron, the cathode and the anode are replaced by the network frequency. This makes the cathode lifetime at AC arc plasmatron at least two times higher than in DC ones.
- In the DC arc plasmatron, ballast resistors are provided for supply stability for arc stability. However, this causes active power losses. In AC arc plasmatrons, reactors are connected in series to provide arc stability.

AC plasmatrons are preferable instead of DC ones because of the advantages mentioned above.

The following paragraphs show a description and the operating principle of three-phase AC plasmatron and also the facility and properties of the high-power alternating current arc-jet plasma torch which was established at AR&TeCS (ARTECS Anadolu R&D Technology Engineering and Consultancy Company, Ankara University Technopolis) are given. In addition, this study covers the measurement techniques used in order to characterize the plasma. In “Results and Discussion” section, the results obtained during the tests are presented.

2. AN ALTERNATING CURRENT PLASMATRON FACILITY

2.1 The design of the plasmatron and operating principle

A new design of three-phase AC plasmatron of “Zvezda”-type (star) is shown in Figure

1. This type plasmatron used for our study is an arc heater of gas heating and consists of the mutual mixing chamber (1) and three identical arc chambers which are connected to each other. This three arc plasmatron has three electrodes instead of six ones. It provides high lifetime and reliability. Also, temperature and pressure distributions are uniform in the plasmatron exit cross section. Each arc chamber includes the end cover (back plate) (2), the chamber– electrode (3) and the constrictor (4). Electrical insulators separate the electrode from the end cover and the constrictor. In the insulators, the working gas (air) is supplied through the tangential orifices to produce a vortex. The heated gas exits the plasma torch through the nozzle of the mixing chamber, whose axis is normal to the plane of the sketch. Also, each electrode is fitted with solenoids (5). The magnetic field of the solenoids causes a rotation of the radial part of the arc. This leads to decrease of the electrode erosion. The electrodes, constrictor, the mixing chamber, and the output nozzles are water-cooled [3].

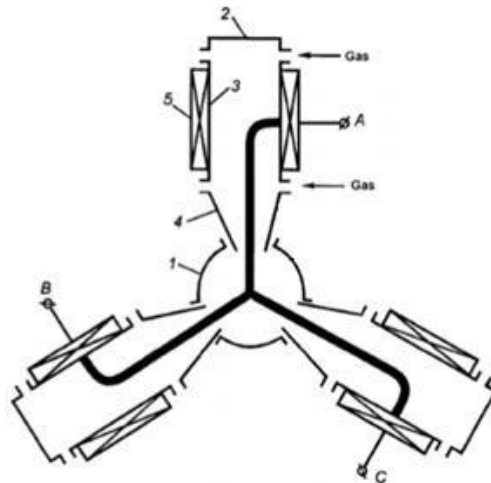


Figure 1: Diagram of the AC Three-phase Plasmatron [7].

The plasmatron is started up as follows. Firstly, water and working gas supply systems are activated. In each arc chamber, the high-frequency low-power discharge is ignited by using a special power source meanwhile a voltage is supplied to the electrodes. The arc passes through the insulator and juts out above the internal surface of the electrode. The applied voltage causes a breakdown in the electrode-constrictor gap where the high-frequency discharge closes with the formation of an arc. Under the effect of the aerodynamic forces, the closing section of the arc is moved downwards along the flow after the main arc is ignited. The ends of the arc at the bottom of the flow are closed by the “star” circuit with the zero point because of all three arc chambers in relation to each other [7].

As in our system, plasma from three

electrodes mixes in the water-cooled mixing chamber. It is opened to the atmosphere using nozzles at different diameters from the mixing chamber. The speed and shape of the plasma varies depending on the pressure difference and the diameter of the orifice.

The high-power arcs produce electrode erosion. As the electrode erosion increases, the service life of the electrodes and plasmatron efficiency decrease. Various methods have been developed to solve the short lifetime of the electrodes. These methods depend on the working gas which is heated in the plasma torch, the magnitude of arc current and gas pressure in the discharge chamber [7]. One of these methods is that an axial magnetic field can be applied to the arc root by a magnetic coil in each electrode [8]. Coating of the electrodes with electrical and thermal resistance materials such as graphite is another method. Further research studies are

needed to mature this method for commercial application.

2.2 Generalized working characteristics of plasma torches

Volt-Ampere Characteristics (VAC) of the arc are the most important electrical characteristics of the plasma torch [7]. Koroteev et al. used the generalized criterial dependence to analyze the experimental data in the plasma torches with vortex stabilization of the arc [9]:

$$UI/Gh_0 = f(I^2/Gd\sigma_0h_0, pd^2/Gh_0^{1/2}) \quad (1)$$

where U is the voltage, I is the current of arc, G is the total flow rate of the gas, p is the pressure in the chamber, and d is the characteristic dimension represented by the mean value between the diameters of the electrode and of the output cross section of the confusor which can be shown as d_m . Also, σ_0 and h_0 are the characteristic values of electrical conductivity and enthalpy of the gas respectively. These two parameters can be accepted as constant.

The group of the determining criteria (independent parameters) is given as:

$I^2/Gd, G/d, pd, BI/pd, I^2/pd^2$ and so on.

Also, the group of the determined criteria (dependent parameters) is defined as: $U, Ed, Ud/I, Ed^2/I, \eta$ and so on.

Zhukov and Zasytkin emphasize that the new criterion $\Pi = I^2pd/G^2\sigma_0h_0^{3/2}$ can be

obtained by multiplying the determining criteria. This includes all the parameters influencing the dependent parameter, that is, arc voltage. For passing through dimensional complexes, $K = UI/G$ and $K_0 = I^2pd/G^2$ are denoted. The expression for the generalized volt-ampere characteristic has the following form $K = f(K_0)$. Complex K_0 which is dependent parameter includes the energy criterion and the Reynolds and Knudsen numbers:

$$K_0 = I^2pd/G^2 = (I^2/Gd)(d/G)(pd) \quad (2)$$

Also, the complex K which is independent parameter contains the energy criterion and the Reynolds number:

$$K = UI/G = U\sqrt{(I^2/Gd)(d/G)} \quad (3)$$

In general, the following dimensions of the quantities are used; $|U| = V, |I| = A, |G| = g/s, |p| = MPa, |d_m| = cm$.

Figure 2 demonstrates the results of processing experimental data obtained on plasma torches of different schemes: the star type, on the simulation single-phase plasma torches and on two plasma torches of the vortex scheme using direct current with a constrictor channel and approximately constant arc length. As seen Figure 2, all points fit quite accurately a single line with a 15 % average deviation of the points from the line.

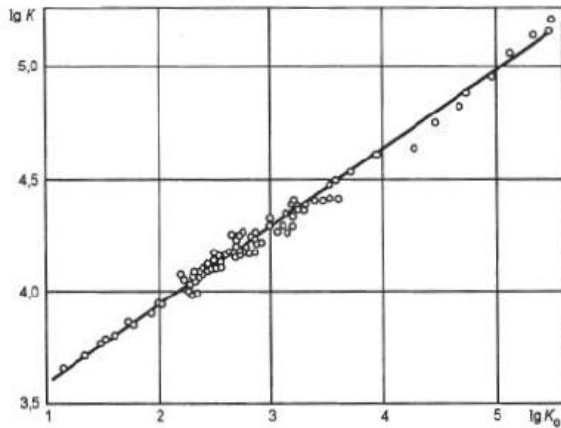


Figure 2: Generalized Volt-Ampere Characteristics [7].

The VAC of the arc U can be shown as following:

$$U = 1.84 \cdot 10^3 (I^2/Gd)^{-0.16} (G/d)^{0.16} (pd)^{0.34} \quad (4)$$

If the SI units are transferred, Equation 4 becomes:

$$U = 732.5 (I^2/Gd)^{-0.16} (G/d)^{0.16} (pd)^{0.34} \quad (5)$$

From Equation 5, the arc voltage (U) is found and then the power can be calculated by using voltage and current values.

Furthermore, the thermal efficiency η which is the fraction of the heat losses in the walls from the power supply to the arc discharges is important to calculate the output parameters of plasma torches. The equation of thermal efficiency is shown in following form [7]:

$$\eta = (I^2 pd_m / G_1^2)^{-0.09} \quad (6)$$

The flow rate of the gas is considered through one phase plasma torch $G_1=G/3$.

In addition to Equation 6, other method is given below to calculate thermal efficiency.

$$\eta = \frac{P - W}{P} \quad (7)$$

where P is the power in the arcs, W is the heat losses ($W=mc(T_{out}-T_{in})$), $P-W$ is the energy for the working gas heating [10].

2.3. The facility

The establishment of the High-Power Plasmatron Test System at AR & TeCS (ARTECS Anadolu R&D Technology Engineering and Consultancy Company, Ankara University Technopolis) facilities has been successfully completed and the qualification tests have been carried out with KeRC cooperation as well. A schematic drawing of a complete plasmatron test system, established a similar one in the AR & TeCS facility is shown in Figure 3. The plasmatron relates to gas arc heaters of megawatt class and the working gas is air. The operation of the plasmatron necessitates the availability of the power supply system, the working gas feed system, the water cooling system, the rooms ventilation system, the hot gas offtake system and the measurement and control system.

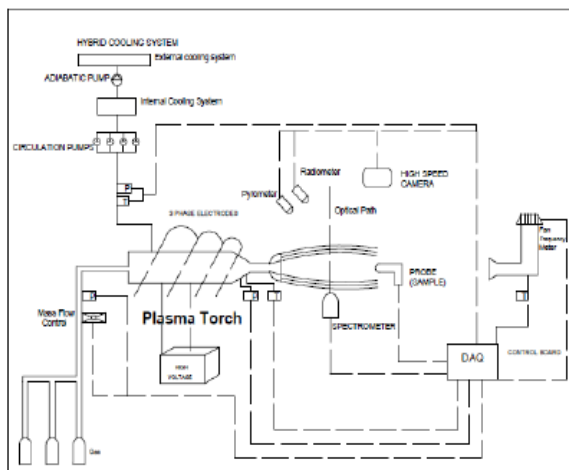


Figure 3: A Schematic Drawing of a Plasmatron Facility

The plasmatron system is decomposed into five subsystems. Details of each subsystem will be described in the following subsections.

Electrical Subsystem

Electrical subsystem provides required current and voltage needs to the system in order to generate plasma arc. As seen from Figure 4, reactive power is compensated after transforming 34.5 kV into 10.5 kV in transformer building. In addition, reactors are used in our system to limit the incoming current to the system properly. Since one reactor is used for each phase, the system consists of in total of three current limiting reactors. To obtain different limited current values, the reactor was designed with multiple hubs for required impedance values.

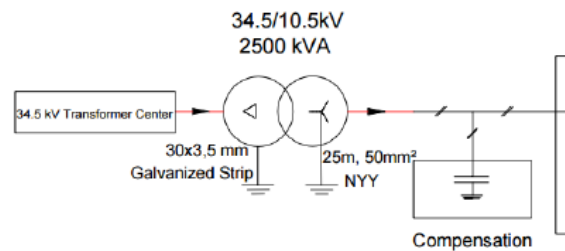


Figure 4: The Plasmatron's Electrical Subsystem.

Cooling Subsystem

Heat loss of a 1 MW plasmatron will be very high and it may harm the system; therefore, a cooling system is needed to decrease the system's temperature, and water is used in this system for cooling. The water cooling subsystem in the facility consists of two parts, internal and external. The internal cooling system, using deionized water because of high voltage risk of the ions in the water is placed inside the laboratory and mainly consists of buffer tanks, system pumps, and circulation pumps. The outer cooling subsystem, using antifreeze to decrease the freezing point of the cooling water below the external air temperature is placed outside and mainly consists of a water tower, a tower fan, and an adiabatic pump.

Gas Feeding Subsystem

Air is used as working gas in the system and needed to be supplied to the system via a gas feeding subsystem. In order to form the plasma continuously, pressure and mass flow of air should be set properly. The gas

feeding subsystem mainly consists of compressed air cylinders, over 200 bar, pressure regulators, actuator, a mass flow controller, and pressure transmitters. The actuator is used to turn the valve on and mass flow controller is used to adjust the air flow. The mass flow rate of the gas is being calculated through venture nozzle.

Ventilation Subsystem

When the system is operated, the temperature of the room may increase and some active radicals and temporary hazardous gases may be formed. In order to exhaust these hot gases from the laboratory and also to decrease the room temperature, a ventilation subsystem is built. According to room temperature, the ventilation subsystem's rotational speed can be adjusted by using inverter system.

Data Acquisition (DAQ) and Control Subsystem

This subsystem both acquires sensor/transducer signals and controls the whole system remotely. Main parts of this subsystem are a PC and a control module. Control module mainly consists of power supplies, sensors, transducers, relays, and a DAQ module which provides a connection with the PC. The software is needed to provide communication between PC and control module and LabVIEW software is used in this system.

Every subsystem above and plasmatron itself are controlled and measured by DAQ

subsystem. No human action is performed after starting the tests, the system is remotely controlled till the end of the tests. Briefly, following operations are performed before generating plasma by using LabVIEW in a controlled way:

- Turning water pumps on
- Turning ventilation on and setting its rotational speed
- Turning actuator on and setting air mass flow
- Turning high voltage on

After performing operations above, plasma is expected to be formed. From the beginning of the program till the end, following input values are measured/calculated and controlled. The min/max constraints for each input are defined for a successful and safe test. In the case of an unexpected value, the system safely turns itself off and reports the source of the unexpected value. For example, the system will safely turn itself off if 9.1 MPa pressure is sensed and min/max values are entered as 3/9 MPa, respectively, for incoming water pressure, and also at the end, user is informed that the system is halted due to high water pressure. Some measured/calculated input values are listed below:

- Current and voltage values
- Plasma power and temperature
- Water temperature
- Water pressures and mass flow
- Air pressure and mass flow

- Room temperature

Since values of each input are measured/calculated, their time graphs can be easily drawn. Figure 5 is an example screen from the system's LabVIEW DAQ and Control program. In this figure, time graphs of plasma temperature, power and water pressure can be seen. And also, there is a STOP button which safely turns the system off when pressed.

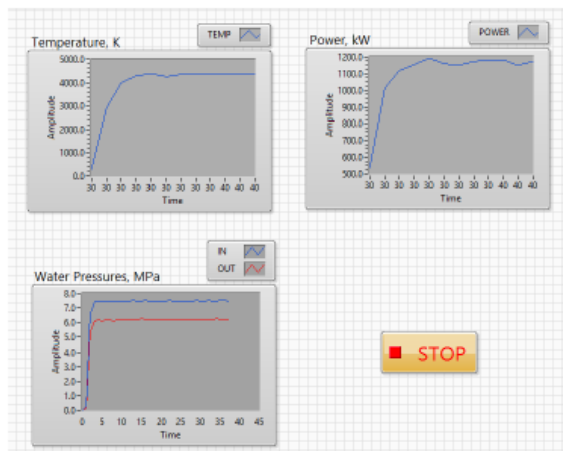


Figure 5: An Example Screen from the System's LabVIEW DAQ and Control Program.

Developed DAQ Control and Measurement Program is an advanced program which gives users to fully control and acquire every data and state of the tests. This program also writes every data of tests into files and allows users to simulate previously performed tests by reading previous test results from those files. Every test data can be observed in these simulations as observed in real tests.

In addition to LabVIEW program, test laboratory is equipped with CCTV cameras and a high-speed high-resolution camera to observe and analyze plasma formation step-by-step.

The schematic drawing of plasmatron is shown in Figure 6. The diameter of plasmatron is approximately 1.13 m.

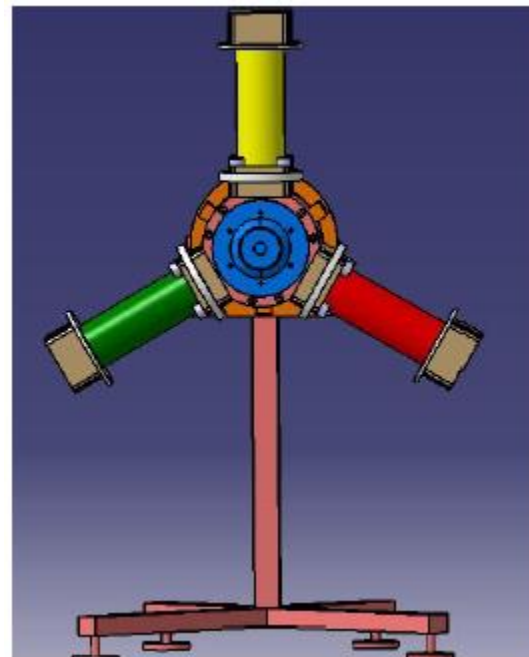


Figure 6: The Schematic Drawing of Plasmatron.

The plasmatron can be operated in high and low power modes. Experiments in the high-power mode are carried out with a current of 200-400 A, with reactor resistance set to $D = 1.4$ cm diameter of the nozzle with 1 MW input power and heat flux is measured by using heat flux probe. In other experiments, the reactor is adjusted and 200-300 A current is given to provide lower-power and

the pressure is measured with a Pitot probe at the exit of the nozzle with $D = 1.4$ cm diameter.

Another image of a 1-MW plasmatron designed at the KeRC is shown in Figure 7.

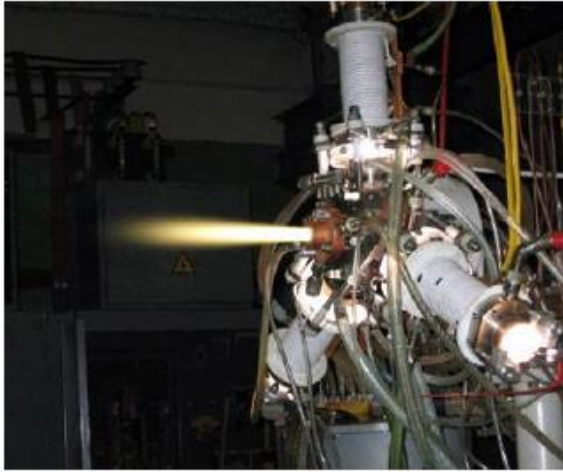


Figure 7: An Image of Arc Jet Plasma Generator.

3. PERFORMANCE MEASUREMENTS

Specific probes, Pitot probe, and heat flux probe have been designed, built and used in arc jet facilities to determine flow properties. Although the intrusive measurements distort the flow, they give much-needed information about the plasma flow. The following sections will present description, working principle, measurement and accuracy of these probes to the reader.

The gas flow rate is calculated by measuring a pressure difference of the venturi nozzle and temperature of the gas in gas collector just before entering the plasma system,

using the following equation.

$$G_g = \frac{m \cdot P_w \cdot F_w \cdot q_1}{\sqrt{T_g}} \quad (8)$$

Here m is a constant value (0.3965), P_w is the pressure of venturi, F_w is area of the venturi $F_w = d_w^2 \cdot \frac{\pi}{4}$, q_1 is also a constant value equal to 1 and T_g is the temperature (288 K) [7].

Also, the mixing chamber pressure is measured directly using pressure transducer and chamber temperature was calculated by using Gas Dynamic Method. According to this method, the following analysis method is coded in the software:

$$f(T_{ch}) = G_g / F_{noz} \cdot P_{ch} \quad (9)$$

Here, f is a function of chamber temperature. G_g is the gas flow rate, F_{noz} is the cross-sectional area of nozzle and P_{ch} is the chamber pressure. The chamber temperature value is expected to be minimum 4000 K.

In addition, with the optical emission spectrometer, the light coming from the plasma flow is taken as a wavelength-intensity graph and the plasma parameters such as electron temperature, particle composition can be determined. The optical spectrometer is a basic tool that can be used for plasma characterization at wide temperature and pressure ranges. Different methods have been developed for plasmas

with different properties in temperature measurement by optical emission spectrometry [11]. The calculation of the electron temperature in the local thermodynamic equilibrium method is made according to the following formulation [12]:

$$\ln \left[\frac{I_2 \lambda_2}{g_2 A_2} \right] = -\frac{1}{kT} E_2 + b \quad (10)$$

where I_2 is the light intensity, λ_2 is the wavelength, g_2 is the statistical weight, A_2 is the transition probability, E_2 is the energy level, k is the Boltzmann constant, T is the excitation temperature and b is a constant. The wavelength and light intensity information are obtained from the graphic, g_2 , A_2 , E_2 values are obtained from National Institute of Standards and Technology (NIST) tables [13].

Taking $\ln \left[\frac{I_2 \lambda_2}{g_2 A_2} \right]$ as the y-axis and E_2 as the x-axis, a slope parameter which is $-1/kT$ can be obtained by fit and then the electron temperature can be obtained.

Moreover, for the observation of the thermal protection materials exposed to plasma flow, optical techniques like pyrometer and radiometer can be used [14]. The pyrometer is a type of remote-sensing thermometer used to measure the surface temperature and the heat flux rate to a surface in radiative equilibrium can be determined. Especially for the material ablation test, a high-speed camera can be used as shown in Figure 3.

In some wind tunnel tests, in order to determine diagnostic information about the flow around the model, schlieren system which is the flow visualization technique can be used. Schlieren system is utilized to visualize the flow away from the surface of an object. In this system, light rays are bent whenever the flow away from the surface of an object [15].

3.1. The Pitot Probe

Pitot probes have been used for a long time in flow phenomena in plasma sources because of low cost and easily performed probe [16]. The Pitot probe which is made from brass is a cylindrical tube with a front hole. Also, it is parallel to the flow. The conceptual sketch and the picture of the Pitot probe are shown in Figure 8 and Figure 9 respectively. It is water-cooled to prevent from its destruction. Thus, its dimensions are large enough to enable effective internal water cooling.



Figure 8: The Conceptual Sketch of the Pitot Probe [1].

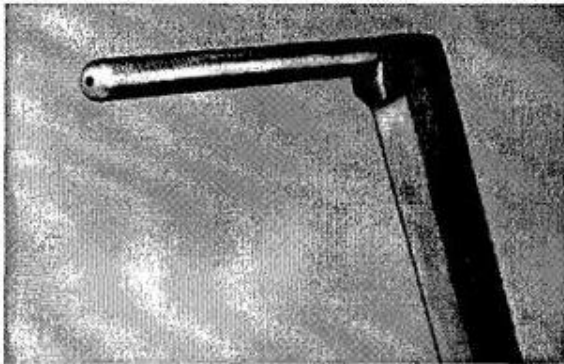


Figure 9: The Picture of the Pitot Probe (left) [1] and the picture of Pitot probe produced by ARTECS based on VKI design.

The Pitot probe measurements can give information about the dynamic or total stagnation pressure of the plasma flow. In addition, it characterizes mass flow rate, symmetry, stability of plasma jet. In measurement accuracy, the impact of friction can be disregarded. Thus, measurement error is very small [17]. As mentioned above, since the probe is cooled to withstand the plasma heat, a big

temperature difference and a thermal boundary layer appear between the probe and the gas flow. This acquires some deviation the pressure estimation; however, this issue appears not to have been extremely known up to this point [18, 19]. Moreover, the proportion between the outer diameter and the orifice diameter has some impact on the measurement and should be considered by a particular coefficient in the outflow of the dynamic pressure [16].

3.2. The Heat Flux Probe

There has been an assortment of heat flux probes improved throughout the years. The heat flux probe is used to determine the local total enthalpy and establish test conditions for materials and structures testing. Also, it allows long-duration and continuous measurements.

The increase of coolant temperature due to cooling of the stagnation region of the probe yields the heat flux by a balance between power inflow from the plasma and power outflow through the water:

$$qS = \dot{m}c_p(T_{out} - T_{in}) \quad (11)$$

where q is the stagnation-point convection heat flux rate, S is surface area of the probe, \dot{m} is the mass flow rate of the water and c_p is the specific heat of the water, T_{in} is the temperature of the inlet water to the cooling surface of the copper surface and T_{out} is the temperature of the water coming out of the cooling surface of the copper surface. The left side demonstrates power brought from

the plasma jet into the probe and the right side shows power evacuated by the cooling circuit of the probe.

The conceptual sketch of the heat flux probe is shown in Figure 10. Heat flux probes utilize very catalytic surfaces to acquire the best repeatability and comparison capability. Thus, copper, which has a relatively high catalytic efficiency, is mostly used at front of the probe [20].

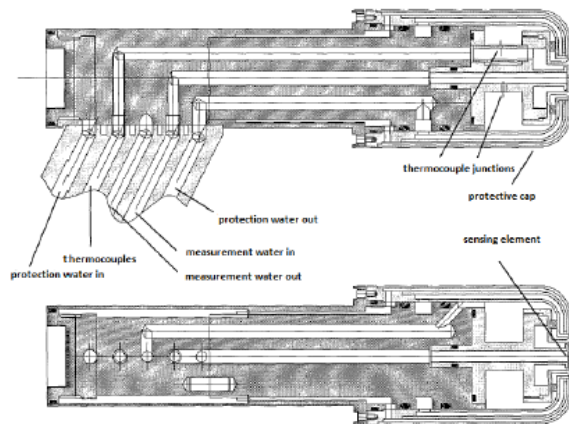


Figure 10: Concept of Heat Flux Probe [1].

The protective cap provides the external geometry of the probe. Its wall is also made from copper. As seen from Figure 10, there are two thermocouple junctions which are part of the same thermocouple. These thermocouple junctions measure the temperature difference ($T_{out}-T_{in}$) [1, 20].

Moreover, because of the very high temperatures, the probes cannot be used for a long time during experiments, in other words, the probes cannot be kept up to

steady - state. However, thanks to the correlation between ΔT and time, we can find ΔT for the infinitive time. In other words, if we find the value of time independent of the probes, we can calculate the correct value of ΔT , heat flux etc.

The following paragraphs explain how to compute the terminal temperature of probe used in plasmatron experiments. Assume that the probe is considered to be lumped mass (no gradients in temperature inside the probe), the temperature of plasma is around 5000 K and radiation is neglected. Under these assumptions, the governing equation can be given as:

$$M c_p \frac{dT}{dt} = hA(T_{plasma} - T) - Q_{out} \quad (12)$$

where M is the mass of the probe, c_p is the specific heat of brass which is the material of the probe. Moreover, h is the heat transfer coefficient between probe and plasma and A is the surface area exposed to plasma flow. Q_{out} is heat loss due to cooling by water circulating inside the probe which can be directly obtained from measurement.

As a solution of the equation above, the temperature of the probe has the following form:

$$T(t) = T_{terminal}(1 - e^{-at}) \quad (13)$$

In the equation above, $T_{terminal}$ can be obtained by considering steady-state conditions; therefore,

$$0 = hA(T_{plasma} - T_{terminal}) - Q_{out} \quad (14)$$

Here the terminal temperature is obtained as:

$$T_{terminal} = T_{plasma} - \frac{Q_{out}}{hA} \quad (15)$$

This equation can be verified by experimental data. Thus, hA can be obtained experimentally. Note that $\alpha = hA/Mc_p$. Now, our purpose is to obtain $T_{terminal}$ and α coefficients by least square fit. However, it should be reformulated to analyze the experimental data more accurately. Let's differentiate the transient equation,

$$\frac{dT}{dt} = \alpha T_{terminal} e^{-\alpha t} \quad (16)$$

This part is important, but we calculate heat flux based on relative less water flux circulating behind the heated surface. This water flux is only used for measurement purposes and so its cooling is neglected. Because of the very high continuous flow rate of plasma gas especially in AC type plasmatron, this cooling effect is very small. Assume that cooling of measurement water is neglected and $T_w^{ave} = \text{constant}$ (average temperature of water). According to these assumptions,

$$\dot{m}c_p^w(\Delta T) = h_w A_w (T - T_w^{ave}) \quad (17)$$

Let's take derivative of the equation above,

$$\frac{d\Delta T}{dt} = \frac{h_w A_w}{\dot{m}c_p^w} \frac{dT}{dt} = \frac{h_w A_w \alpha T_{terminal}}{\dot{m}c_p^w} e^{-\alpha t} \quad (18)$$

Let's take logarithm of both sides;

$$\log\left(\frac{d\Delta T}{dt}\right) = \log\left(\frac{h_w A_w \alpha T_{terminal}}{\dot{m}c_p^w}\right) - \alpha t \quad (19)$$

After obtaining α , it is known that ΔT has the following form where a and b are constants:

$$\Delta T = a + b(1 - e^{-\alpha t}) \quad (20)$$

3.3. The Langmuir Probe

In the next step of the computation, the heat flux can be calculated as in Equation 11.

The Langmuir probe is widely used plasma diagnostics and it characterizes plasma to determine the physical properties of the plasma. It is a device used to measure some basic properties of plasmas such as electron temperature, electron density, and electric potential of plasma, floating potential, ion current density, and electron energy distribution function. It comprises of sticking a wire into the plasma and measuring the current to it at different applied voltages [21].

4. RESULTS AND DISCUSSION

The experiments were carried out with using the three dimensions of exit nozzles having the throat diameters changing in the range of 10 mm to 35 mm, named from smallest to

largest respectively “S”, “M” and “L”. The plasmatron operating parameters were

350 A, the flow rate of the working gas (air) was varied in the range 100 to 200 g/s. Comparative test parameters of the plasmatron with differing exit nozzles are placed in Table 1.

The arc current and the arc voltage are measured during the test using a standard type of network analyzer. As it can be seen in Figure 11 and Figure 12, current values are stable being independent parameter around adjusted values, but the voltage is not since it is a main dependent parameter of plasmatron. This is suitable for the character of discharge voltage of the plasma system as explained above.

determined in different modes, where the arc currents were varied within the range 230 to

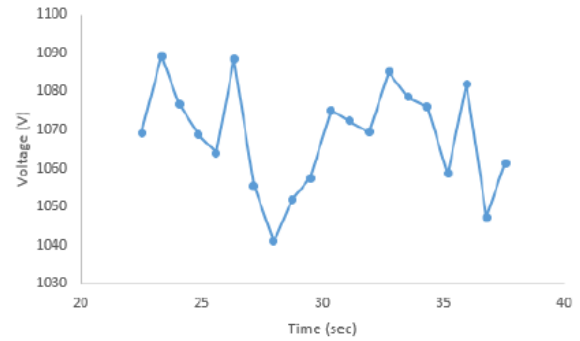


Figure 11: The graph of Voltage versus Time.



Figure 12: The graph of Current versus Time.

Table 1: Parameters of the Plasmatron with Various Exit Nozzles.

No	Gas Flow Rate [g/s]	Arc Current [A]	Arc Voltage [V]	Power [kW]	Chamber Temperature [K]	Chamber Pressure [bar]	Nozzle Types
1	137	236	1270	900	3940	14.90	S
2	118	243	1045	760	4000	6.40	M
3	137	330	860	850	3770	3.20	L

With respect to the Table 2, all tests were performed using the nozzle with the throat section of 14 mm for air as a working gas. These data were acquired on the different plasmatrons varied from each other by an arc voltage, arc current, gas flow rate, power, chamber temperature and pressure and so on. Plasmatron disassembly after the

check tests has revealed the inner surfaces of the construction including the ignition units of arc discharges are serviceable. In addition, the chamber temperature mostly exceeds 4000 K at high-power (above 1 MW) as it can be seen from Table 1 and Table 2.

Table 2: Characteristics of the Plasmatron.

No	U [V]	I [A]	G_g [g/s]	W [kW]	T_{ch} [K]	PL_{in} [bar]	PL_{out} [bar]	P_w [bar]	P_{col} [bar]	P_{ch} [bar]
1	1060	330	128	1050	4500	10.80	9.30	27.90	17.90	15.40
2	1130	328	143	1110	4310	11.20	9.70	31.20	30.00	16.60
3	1110	318	134	1060	4400	12.00	10.50	29.20	19.10	15.80
4	1250	325	125	1200	4300	7.32	5.97	26.93	19.65	14.28
5	1260	325	130	1200	4400	7.60	6.30	28.32	20.91	15.34
6	1065	325	104	1040	4460	7.53	6.24	22.70	16.78	12.41
7	1260	184	101	707	3718	7.49	6.19	21.93	15.11	10.55
8	1200	312	127	1153	4281	7.54	6.22	27.71	20.08	14.70
9	1222	325	125	1175	4382	7.53	6.25	27.23	20.09	14.70
10	1235	325	125	1180	4400	7.56	6.25	27.21	19.98	14.73
11	1070	325	103	1043	4528	7.49	6.21	22.52	16.67	12.45
12	1065	325	108	1034	4130	7.46	6.14	23.48	16.48	12.14
13	1670	193	145	971	3697	7.45	6.15	31.71	21.88	15.20
14	1576	196	140	930	3800	7.46	6.13	30.26	21.10	14.77

U – average arc voltage; I – average arc current; G_g – gas flow rate; W – power; T_{ch} - chamber temperature; PL_{in} – pressure in the inlet water manifold; PL_{out} – pressure in the outlet water manifold; P_w – gas pressure upstream of the Venture-type nozzle; P_{col} – gas pressure in the air manifold; P_{ch} – chamber pressure.

Apart from the chamber pressure, the plasma torch pressure was measured as about 1.5 MPa using Pitot probe and pressure transducer. Plasma pressure can change depending on the distance of the Pitot probe from the nozzle exit and it is measured with a distance from the plasma 30 cm.

Heat flux values are calculated by measuring flow rate and temperature differences of the cooling water using Equation 11. The heat flux values were over 5.9 Mcal/kg·m² and changed depending on the place of the probe. This change will be formulated with

the following studies, making more tests. Since there is an erosion of copper electrode, this may cause some catalytic effects for the recombination of the active atoms or small molecules. This recombination and establishment of the new bonds will increase energy on the probe, resulting some degree of the heat flux values.

Also, the efficiency of the plasmatron was calculated about 75 – 80 %. To obtain efficiency of the plasmatron, Equation 6 and Equation 7 were used. For given equations, the results of efficiency of the plasmatron are presented in Table 3.

Table 3: The thermal efficiency values obtained during some tests.

<i>No</i>	<i>P</i> [kW]	<i>m</i> [g/s]	<i>T_{in}</i> (°C)	<i>T_{out}</i> (°C)	<i>η</i>
1	1101.79	6.583	16.96	27.16	0.745
2	1011.77	6.046	23.82	33.52	0.757
3	1037.73	5.806	23.85	33.46	0.761
4	1128.47	5.773	23.46	33.88	0.777

5. CONCLUSION

Plasmatrons are high-temperature gas sources. They are used in aerospace technology development such as subsonic and supersonic gas flow modeling, thermal insulation materials and component testing. They are also utilized in scientific research, in the technological process of obtaining new materials, in ultra-basalt and nano fibers, in surface treatments, in wastes

utilization.

The detailed design of the star type plasmatron and its auxiliary electrical, air and cooling subsystems was investigated and improved in the AR&TeCS facility. The operation characteristics of the facility, the mixing chamber pressure, chamber temperature and two main intrusive measurement techniques (Pitot probe and

the calorimetric heat flux probe) were briefly described in this paper. Also, the experimental studies were presented. At an operation with air as a working gas, the following maximum characteristics were achieved: chamber temperature 4460 K, chamber pressure 12.41 bar, and power 1040 kW.

An important electrical characteristic of the plasma torch is Volt – Ampere Characteristic (VAC). $K=f(K_0)$ is the expression of generalized VAC and according to Figure 2, all points fit quite accurately a single line, which is confirmed with our experiments. Also, the voltage is a main dependent parameter of plasma torch, so voltage values are not stable due to the character of the discharge mechanism and total fluctuation from all effecting parameters. However, current values are stable because current is independent parameter around adjusted values. This phenomenon which is suitable for the discharge voltage characteristic verified with our experiments as seen in Figure 11 and Figure 12.

The experimental studies show that the star type plasmatron has many advantages mentioned below. Thus, our plasmatron system has unique and superiority properties compared to other plasmatron systems.

- They operate with three-phase industrial current without the need for transformer, rectifier and frequency converter.

- The modular structure and the exchange of electrodes are easy.
- There is a uniform distribution of the pressure and temperature at the nozzle exit.
- The electrodes have a long lifetime.

The application of plasmatron and its technology is mostly dependent on the electrodes lifetime. The high-power arcs produce electrode erosion if there is no additional precaution against high energy electron and ions collisions on the electrodes. As the electrode erosion increases, the service life of the electrodes and plasmatron efficiency decrease timely. The lifetime of the electrodes will increase at least twice since anode and cathode change continuously in alternating current. One of the main methods to reduce the electron erosion is to apply an axial magnetic field to the arc root by a magnetic coil in each electrode. The other method is that coating the electrodes with electrical and thermal resistance materials such as graphite.

REFERENCES

- [1] Bottin, B., Chazot, O., Carbonaro, V., Van Der Heagen, V., Paris, S. The VKI plasmatron characteristics and performance. *North Atlantic Treaty Organization*. 1999.
- [2] Pessin, M., Butler, J., Sparks, J. S. (2009) Thermal Protection System. Retrieved February, 2017 from <https://www.nasa.gov/centers/johnson/pdf/5>

84728main_Wings- ch4b- pgs182-199.pdf

[3] Svirchuk, Y. S., Golikov, A. N. Three-phase Zvezda- type plasmotrons. *IEEE Transactions on Plasma Science*, Vol. 44, No. 12, 2016. 3042-3047.

[4] Katırcıoğlu, T. Y., (2014). Kömür Gazlaştırma. *Plazma Teknolojileri* (155-167) Ankara, Ürün Yayınları

[5] Karpenko, E. I., Karpenko, Yu. E., Messerle, V. E., Ustimenko, A. B. (2009). Use of plasma fuel systems at thermal plants in Russia, Kazakhstan, China, and Turkey. *High Energy Chemistry*, Vol.43, No. 3, 224-228

[6] Fabry, F., Rehmet, C., Rohani, V., Fulcheri, L. Waste gasification by thermal plasma: a review, waste and biomass valorization, (2013). 4 (3), 421-439.

[7] Zhukov, M. F., and Zasyplin, I. M. Thermal plasma torches design, characteristics, applications. Cambridge International Science Publishing. (2007). 399-410.

[8] Yamada, T., and Inatani, Y. Arc heating facility and for planetary entry test technique missions, *The Institute of Space and Astronautical Science Report SP* (2003). No. 17.147-163.

[9] Koroteev, A. S., Mironov, V. M., and Svirchuk, Y. S. Plasmotrons-design,

characteristics, calculations, (in Russian). Moscow:Mashinostroenie, (1993). 296.

[10] Rutberg, Ph G., Safronov, A. A., Popov, S. D., Surov, A. V., Nakonechny, Gh. V. Multiphase stationary plasma generators working on oxidizing media. *Plasma Phys. Control. Fusion* 47 (2005) 1681 – 1696.

[11] Özge Yazıcıoğlu, T. Yaşar Katırcıoğlu, Beycan İbrahimoglu, “Optik Emisyon Spektrometre Kullanarak Yüksek Güçlü Bir Plazmatron Plazma Akışı Sıcaklık Ölçümü”, Sürdürülebilir Havacılık Araştırmaları Dergisi, SÜHAD, Cilt 2, Sayı 1, 2017

[12] Xiao-Zhi, S., Ping, Y., Hua-Ming, Z., and Jie, W. Transition probabilities for NII 2p4f–2p3d and 2s2p23d–2s2p23p obtained by a semiclassical Method. *Chinese Physics*, (2007). Vol 16 No 10, 16(10)/2934-04

[13] National Institute of Standards and Technology. Retrieved February, 2017 from <https://www.nist.gov/pml/atomic-spectra-database>

[14] Chazot, O., Panerai, F., Muylaert, J. Catalysis phenomena determination in plasmatron facility for flight experiment design. *48th AIAA Aerospace Sciences Meeting Including the New Horizons Forum and Aerospace Exposition*. (2010).

[15] Hall, N., (2015). Schlieren system. Retrieved February, 2017 from

<https://www.grc.nasa.gov/WWW/K-12/airplane/tunvschlrn.html>

[16] Chazot, O., Gomes, J. M. P., Carbonaro, M. Characterization of a “Mini-plasmatron” facility by pitot probe measurements. *American Institute of Aeronautics and Astronautics, Inc.*

[17] Ristic, S., Isakovic, J., Ilic, B., Ocokoljic, G. (2004). Review of methods for flow velocity measurement in wind tunnels. *Scientific-Technical Review*, (1998). Vol. LIV, No. 3, 60-71.

[18] Hare, A. L. Velocity measurement in plasma flows using cooled pitot tubes: an unsolved problem. (1977). *Proceedings of the 3rd International Symposium on Plasma*

Chemistry, G3.1, Limoges.

[19] Porterie, B., Larini, M., Loraud, J-C. Cooled pitot tube in plasma jet: an impact-pressure recovery model. (1994). *Journal of Thermophysics and Heat Transfer*, Vol. 8, No. 3. 385-392.

[20] Lumens, J. F. Bottin, B., Carbonaro, M. Design of a steady-state heat flux probe for measurements in an induction-heated plasma flow [wind tunnels]. ICIASF'97 Record. *International Congress on Instrumentation in Aerospace Simulation Facilities*, 410-419.

[21] Chen, F. F. (2003). Langmuir probe diagnostics. Retrieved February, 2017 from <http://www.seas.ucla.edu/~ffchen/Publs/Chen210R.pdf>